ter yields values larger by 3 seconds for the former and smaller by 3 seconds for the latter. These differences, which have not yet been resolved, correspond to the interval during which the most significant thruster activity (the reduction of orbital period by 0.02 hour) took place.
7. H. B. Neimann, R. E. Hartle, W. T. Kasprzak, N. W. Spencer, D. M. Hunten, G. R. Carignan, *Science* **203**, 770 (1979).
8. The scale height, H, is related to the absolute temperature, T, by $H = RT/\mu g$, where R is the universal gas constant, μ is the mean molecular weight, and g is the local acceleration of gravity.
9. Conversion to solar phase (that is, Sun-Venus-periapsis angle) as the independent variable can be accomplished easily with the use of the data in Table 1.
10. The value of density for periapsis No. 31 (see Fig. 1b) may be significantly in error because of the effects of the thruster activity that just preceded this epoch.
11. C. Boyer and H. Camichel, *Ann. Astrophys.* **24**, 53 (1961); B. C. Murray *et al.*, *Science* **183**, 1307 (1974).
12. I. I. Shapiro, W. M. DeCampli, D. B. Campbell, *Astrophys. J.*, in press.
13. All determinations of ΔP were made from analysis of the radio tracking data by the Pioneer Venus orbiter navigation team at the Jet Propulsion Laboratory, headed by one of us (W.E.K.); no tracking data have yet been received for analysis by the Pioneer celestial mechanics experimenters. This report describes one phase of research carried out at the Jet Propulsion Laboratory, California Institute of Technology, under contract NAS 7- 100 sponsored by NASA. The experimenters at the Massachusetts Institute of Technology were supported in part by contract NAS2-9483 with the NASA Ames Research Center.

16 January 1979; revised 19 January 1979

Ultraviolet Spectroscopy of Venus: Initial Results from the Pioneer Venus Orbiter

Abstract. *Ultraviolet spectroscopy of the Venus cloud tops reveals absorption features attributed to sulfur dioxide in the atmosphere above the cloud tops. Measurements of scattered sunlight at 2663 angstroms show evidence for horizontal and vertical inhomogeneities in cloud structure. Images of the planet at* SO_2 *absorption wavelengths show albedo features similar to those seen at 3650 angstroms from Mariner 10. Airglow emissions are consistent with an exospheric temperature of* ~ 275 *K, and a night airglow emission has been detected, indicating the precipitation of energy into the dark thermosphere.*

The Pioneer Venus orbiter carries an ultraviolet spectrometer mounted with its line-of-sight offset 60° from the south-pointing spin axis. The instrument is a 125 mm, *f*/5 Ebert-Fastie design with a Cassegrain telescope and two detectors, sensitive from 1100 to 2000 Å and from 2000 to 3400 Å, respectively. The spectral resolution is 13 Å; further details have been described (*1*). The instrument operates both in a spectrometer mode, with its diffraction grating scanning, and in a photometer mode, with the grating fixed. We report here preliminary results concerning cloud spectroscopy, scattering, and imaging; day and night airglow emissions; and the atomic hydrogen corona.

Spectroscopy of the cloud layer is attempted only near periapsis, when changes in the illumination, emission, and phase angles during the motion of the diffraction grating are minimized. The ratio of two spectra obtained on different orbits, but with similar observing geometries, is shown in Fig. 1. Their ratio is dominated by two broad absorption features near 2100 and 2800 Å, attributable to the presence of SO_2 in the atmosphere above the cloud tops. If the control spectrum (from orbit 7) is assumed to contain no SO_2, then the depth of the absorption in the 2650 to 2800 Å region implies the presence of about 1×10^{17} cm^{-2} SO_2 in the spectrum from orbit 4. This column density is within the range reported by Barker (*2*). We observe both spatial and temporal variations in this phenomenon.

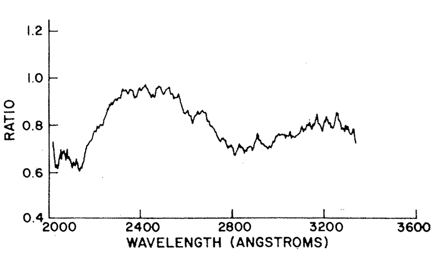

Fig. 1 The ratio of a cloud spectrum taken near the equator on orbit 4 to one taken near 60°N on orbit 7. The optical angles for the two spectra were very similar. The two broad absorption features centered near 2100 Å and 2800 Å are well matched by broad maxima in the absorption cross section of sulfur dioxide.

Figure 2 compares the reflectivity at 2663 Å, measured on a trace across the cloup tops near periapsis on orbit 3, with a scattering model. The model contains a homogeneous sulfuric acid cloud (*3*) overlain by 5 mbar of clear CO_2, and also takes account of the relevant geometric and instrument parameters and of the solar flux. Other traces are best fitted by variations of this model; for example, one including an absorbing layer (*4*) chosen to be consistent with measurements of the net solar flux within the clouds (*5*). We conclude that existing cloud structure models based on measurements at wavelengths > 3000 Å are generally compatible with our data, and that the evidence prior to the Pioneer Venus mission for vertical and horizontal structure inhomogeneities is similarly confirmed.

Images of the planet can be constructed by treating the instrument (in its fixed-grating mode) as a spin-scan camera, in the manner of the Pioneer 10 and 11 polarimeter experiments. Two such images of the southern part of Venus, viewed at half phase on orbit 8, are shown in Fig. 3. These images have been processed to show both the isophotes on the sunlit disk and the weak signal from the dark disk and limb (see below). Our simple rectification procedure presents the planet as it would be seen from 30°N ecliptic latitude. In Fig. 3, the equator crosses the central meridian about one-half radius up from the southern limb and intersects the eastern and western limbs near the top of the images.

Images from several orbits show variable bright and dark features that are generally reminiscent of the markings seen at 3650 Å from Mariner 10 (*6*). On orbit 8, images of the sourthern half of the planet were made at both 2068 Å, where SO_2 absorbs, and at 3297 Å, where it does not (Fig. 3). The isophotes at 3297 Å are smoother than those at 2068 Å. This suggests that the albedo markings seen at 2068 Å show the presence of varying amounts of SO_2 above the scattering cloud layer; this could be due either to true variations in the SO_2 abundance or to variations in the pressure at the cloud tops.

Prominent emissions in the vacuum ultraviolet airglow spectrum occur at wavelengths associated with atomic hydrogen (1216 Å) and atomic oxygen (1304 Å and 1356 Å). Figure 4 compares a disk trace taken at 1304 Å within 1 minute of periapsis (195 km) on orbit 4 with models assuming an exospheric temperature of 275 K and 4 percent T_∞ at 140 km. The lower curve shows that resonance scattering of solar photons and photoelectron impact on T_∞ are together

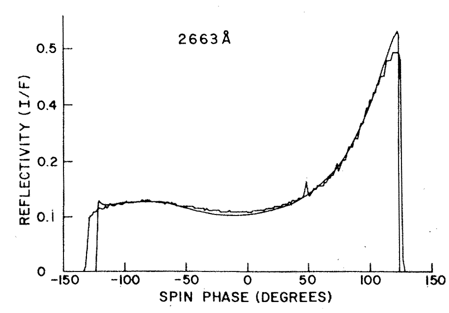

Fig. 2. A trace across the lighted disk taken at 2663 Å on orbit 3. The measurements (irregular line) are well matched by a model (smooth line), with the use of a homogeneous layer of sulfuric acid droplets underneath a 5-mbar layer of clear carbon dioxide.

0036-8075/79/0223-0777$00.50/0

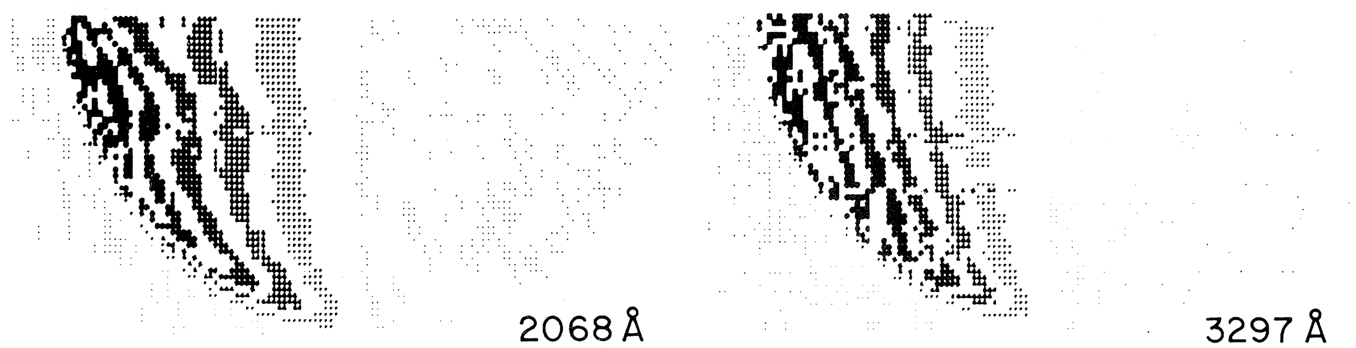

Fig. 3. Images of the southern half of the planet obtained on orbit 8 at 2068 Å and 3297 Å. The images have been processed to show isophotes on the sunlit disk and to emphasize the weak signal from the dark disk and limb at 2068 Å.

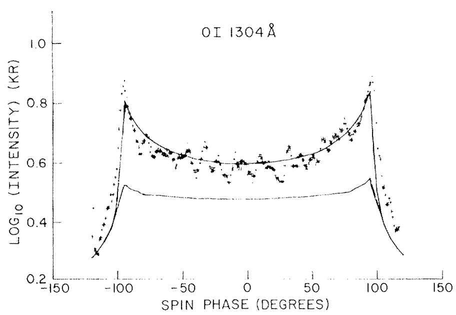

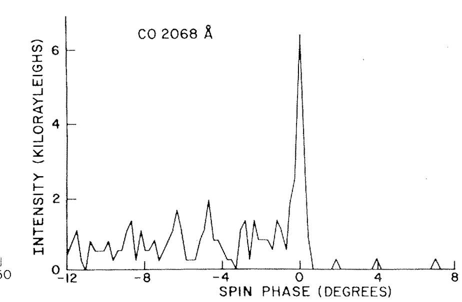

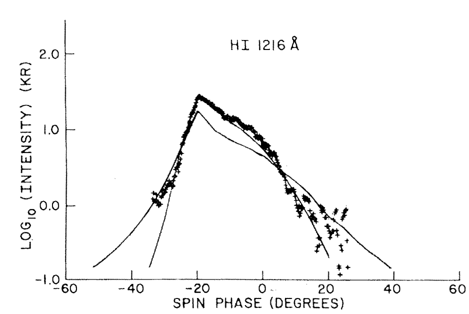

Fig. 4 (left). Sum of two 1304 Å disk traces (pluses) taken near periapsis on orbit 4, as a function of spacecraft spin phase. The lower curve is the calculated intensity in the atomic oxygen (^3p-^3s) resonance triplet due to resonance scattering of solar photons and to photoelectron impact, for a model containing 4 percent O at 140 km. The upper curve contains an additional normalized contribution due to dissociative excitation of CO_2 (the true source of this component is probably CO). Fig. 5 (middle). Average of eight 2068 Å traces crossing the dark limb in the southern hemisphere on orbit 8; the abscissa is spacecraft spin phase measured from the dark limb. The emission is identified as the (0,0) Cameron band in CO; the 6 kR dark limb signal is 4 percent of the signal on the sunlit limb measured on orbit 7. Fig. 6 (right). Four traces at 1216 Å (pluses). They were taken 1 hour before periapsis on orbit 4, at a range of about 19,000 km. The smooth curve in good agreement with the data is calculated from a model having an exospheric temperature of 275 K and hydrogen density at the exobase of 2×10^5 cm^{-3}. For the other curve these parameters are 500 K and 5×10^4 cm^{-3}.

insufficient to explain either the overall intensity or the degree of limb brightening. The upper curve shows that the discrepancy can be made up by a suitably normalized dissociative source. Differences in intensity and degree of limb brightening between our data and similar measurements on Mars (*7*) rule out CO_2, and we attribute the dissociative source to CO, which is much more abundant on Venus than on Mars (*8*).

An ultraviolet emission was detected on the dark limb of Venus from Mariner 5 (*9*). The 2068-Å images in Fig. 3 (and on the cover) show a weak signal on the dark disk; the dark limb is clearly defined, consistent with a limb-brightened airglow emission (the weak signal off the bright limb in this image is due to the wings of the slit function). Bright limb profiles at the same wavelength on orbit 7 also show a prominent airglow emission. By analogy with the Martian airglow (*10*), we identify this emission as the (0,0) band of the CO Cameron bands. The presence of the emission on the nightside indicates a mechanism precipitating energy into the nightside thermosphere. The dark limb signal is ~ 6 kilorayleighs (Fig. 5), compared to ~ 150 kilorayleighs on the bright limb; a nightside energy deposition rate of the order of 0.1 erg cm^{-2}sec^{-1} is indicated. The emission is spatially and temporally variable, and the mechanism presumably involves the interaction of the solar wind with the planet.

The spacecraft's highly eccentric orbit is extremely well suited to the study of the hydrogen corona. Figure 6 shows measurements from four successive equatorial traces taken 1 hour before periapsis on orbit 4. Two models are shown, one with $\langle T_\infty \rangle$ = 275 K and a hydrogen density at the critical level of n_c (H) = 2×10^5 cm^{-3} and one with T_∞ = 500 K and n_c (H) = 2×10^4 cm^{-3}. The 275 K model is an excellent fit, and the 500 K model can be dismissed. Thus, the present results are in good accord with those from the analyses of Mariner 5 data (*11*) in that the deduced T_∞ is ~ 275 K and the critical-level density of hydrogen is 1×10^5 to 2×10^5 cm^{-3}. The associated thermal escape of H is very low, and it is interesting that, given even the highest estimates (*12*) of the nonthermal escape rate (~ 10^7 cm^{-2} sec^{-1}) of H and given the measurement of ~ 0.1 percent H_2O in the lower atmosphere (*13*), the time constant for loss of hydrogen at present is ~ 20 billion years, substantially longer than the age of the planet. Thus, if Venus ever possessed a large amount of water, it cannot have lost it by escape mechanisms known to be operating now.

A. I. STEWART
University of Colorado, Boulder 80309
D. E. ANDERSON, JR.
Naval Research Laboratory, Washington, D.C. 20375
L. W. ESPOSITO
C. A. BARTH
University of Colorado, Boulder

References and Notes

1. L. Colin and D. M. Hunten, *Space Sci. Rev.* **20**, 451 (1977).
2. E. S. Barker, Abstract, DPS/AAS meeting, Pasadena, October 1978.
3. J. E. Hansen and J. W. Hovenier, *J. Atmos. Sci.* **31**, 1137 (1974).
4. L. Travis, *ibid.* **32**, 1190 (1975).
5. M. G. Tomasko, L. R. Doese, J. Palmer, A. Holmes, W. Wolfe, N. D. Costillo, P. H. Smith, *Science* **203**, 795 (1979).
6. B. C. Murray, M. J. S. Belton, G. E. Danielson, M. E. Davies, D. Gault, B. Hapke, B. O'Leary, R. G. Strom. V. Suomi, N. Trask, *ibid.* **183**, 1307 (1974).
7. D. J. Strickland, A. I. Stewart, C. A. Barth, C. W. Hord, A. L. Lane, *J. Geophys. Res.* **78**, 4547 (1973).
8. H. B. Niemann, R. E. Hartle, W. T. Kasprzak, N. W. Spencer, D. M. Hunten, G. R. Carignan, *Science*, **203**, 770 (1979); U. von Zahn, D. Krankowsky, K. Mauersberger, A. O. Nier, D. M. Hunten, *ibid.* p. 768; G. E. Thomas, *J. Atmos. Sci.*, **28**, 859 (1971).
9. C. A. Barth, J. B. Pearce, K. K. Kelly, L. Wallace, W. G. Fastie, *Science* **158**, 1675 (1968).
10. A. I. Stewart, *J. Geophys. Res.* **77**, 54 (1972).

11. D. E. Anderson, Jr., *ibid*. **81**, 1213 (1976).
12. I. Ferrin, thesis, University of Colorado (1976); S. Kumar, D. M. Hunten, A. L. Broadfoot, *Planet. Space Sci*. **26**, 1063 (1978).
13. V. I. Oyama, G. C. Carle, F. Woeller, J. B. Pollack, *Science* **203**, 802 (1979).
14. This work was performed under NASA contracts NAS 2-8816 and NAS 2-9477. We acknowledge the contributions to this experiment of the Pioneer Project Office, our colleagues on the Pioneer Venus Science Steering Group, and especially our colleagues and staff at the University of Colorado's Laboratory for Atmospheric and Space Physics. The false-color image on the cover of this issue was made at Infomap, Inc., Boulder, Colo.

16 January 1979

Infrared Remote Sounding of the Middle Atmosphere of Venus from the Pioneer Orbiter

Abstract. *Orbiter infrared measurements of the Venus atmosphere in the 60- to 140-kilometer region show very small diurnal temperature differences near the cloud tops, increasing somewhat at higher levels. The seasonal (that is, equator to pole) contrasts are an order of magnitude larger, and the temperatures unexpectedly increase with increasing latitude below 80 kilometers. An isothermal layer at least two scale heights in vertical extent is found near the 100-kilometer altitude, where the temperature is about 175 K. Structure is present in the cloud temperature maps on a range of spatial scales. The most striking is at high latitude, where contrasts of nearly 50 K are observed between a cold circumpolar band and the region near the pole itself.*

The Venus orbiter radiometric temperature experiment (VORTEX) on the Pioneer orbiter is an infrared radiometer with ten spectral channels in the wavelength region from 0.2 to 60 μm, similar in concept to Earth weather satellite instruments. Its principal attribute is the ability to measure thermal emission from the atmosphere at eight different, distinct height levels, and thus allow the vertical temperature structure to be recovered. Previous radiometers on U.S. and Soviet missions were simple cloud top mappers, without the ability to discriminate true atmospheric temperature structure from cloud morphology, and with little or no vertical coverage. The height range covered by VORTEX, in contrast, is about 60 to 140 km. This includes the "Earth-like" range of temperatures and pressures; the region of the ultraviolet markings, which exhibit much dynamical activity including the "4-day" circulation; the peak of the ionosphere, and the base of the exosphere. The temperature sounding channels all are in or near the ν_2 fundamental band of carbon dioxide. Two other channels measure reflected solar energy in the near infrared, and one is located in the far infrared near 50 μm. The instrument and its measurement capabilities have been described (*1*, *2*).

Since orbital insertion on 4 December, the radiometer has been activated in all three of its operating modes: global mapping, local imaging, and limb scanning. Excellent performance has been obtained in each case. The second and third of the modes listed require very high data rates and therefore can be used only infrequently without impacting the return from the other science experiments. Consequently, most of the VORTEX data so far are in the relatively low spatial resolution mapping mode (maximum spatial resolution approximately 20 km), and our report deals exclusively with this. The presentation of results from the solar reflectance channels is also deferred until a preliminary analysis has been performed.

Data from orbit 1 are presented in several forms in three figures. Figure 1 shows temperature profile retrievals for selected regions representing dayside (afternoon) equatorial, nightside (predawn) equatorial, and polar soundings. Figure 2 shows a cross section of the atmosphere in the northern hemisphere, consisting of measurements of the temperature at six different height levels from equator to equator over the pole. This plot was made by selecting from the data set those soundings with near-nadir viewing geometry. Figure 3 is a rectangular coordinate map of Venus which has been enhanced in the image processing laboratory to bring out the structure of the cloud tops. The data shown represent a ratio of the intensity in the 11.5-μm window channel to that measured in the wing of the 15-μm CO_2 band, which measures the atmospheric temperature above the clouds near 80 km altitude. This ratio process removes, to first order, horizontal atmospheric temperature differences and viewing geometry effects, and leaves inhomogeneities in cloud opacity or height in the presence of a vertical temperature gradient as the principal source of contrast. The narrow strip to the bottom left is the data taken near periapsis, the width of the strip representing the distance between the horizons to either side of the spacecraft as it passes close to the planet.

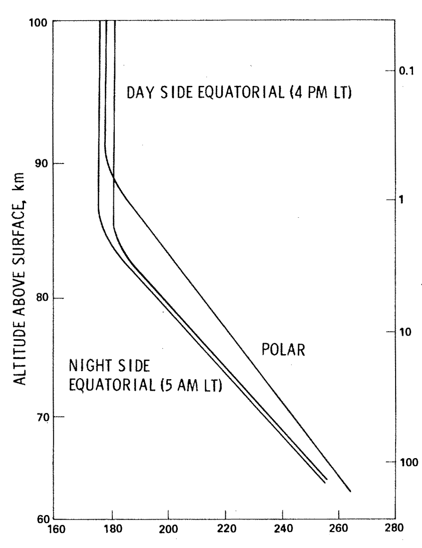

Fig. 1. About 4000 vertical temperature profiles were measured on orbit 1; these three are typical of the equatorial and polar profiles at the local times of day shown. The 11.5-μm window temperature, corresponding approximately to the temperature at unit optical depth in the clouds, occurs at an altitude of approximately 68 km on the dayside and about 0.5 km lower on the nightside. The altitude scale is derived, assuming a reference height of 52 km at 1 bar. [From *NASA SP-8011* (1972)]

The principal conclusions so far from these and similar data from the first few orbits are as follows:

1) Over the limited range of longitudes observed so far, day-to-night temperature contrasts are very small. From about 65 to 80 km, the differences appear to be about 1 K on average at all heights. Between 80 and 100 km, about 5 K of contrast is observed, with the dayside warmer.

2) Pressure modulator radiometer measurements (*1*) near 100 km at the equator show virtually no limb darkening. This implies temperatures constant to within 1 K over a vertical range of at least two scale heights (about 8 km) in this region.

3) The source function for cooling to space at altitudes near 125 km and above is extremely low, at least near the poles where the orbital geometry allows us to measure it (*1*).

4) The cloud top brightness temperatures are about the same on average for measurements made near 5 a.m. and 4 p.m. Venus local time. This result should be compared with figure 8 of Ksanfomality *et al*. (*3*), who interpreted Venera 9 and 10 measurements in terms of 10 K higher equatorial cloud temperatures all over the nightside, relative to the day.

5) Equator-to-pole temperature con-

0036-8075/79/0223-0779$00.50/0